Testing the Top-Down Model Inversion Method of Estimating Leaf Reflectance Used to Retrieve Vegetation Biochemical Content Within Empirical Approaches

Anita Simic, Jing M. Chen, Sylvain G. Leblanc, Andrew Dyk, Holly Croft, and Tian Han

***Abstract*—A top-down model inversion method of estimating leaf reflectance from hyperspectral remote sensing measurements has been tested with an empirical approach used to estimate chlorophyll content. Leaf reflectance is obtained by inverting a geometric-optical model, 5-Scale, validated using hyperspectral AVIRIS data. The shaded scene fractions and the M factor, which includes both the multiple scattering effect and the shaded components, are computed for inverting canopy reflectance into leaf reflectance. The inversion is based on the look-up tables (LUTs) approach. The simulated leaf reflectance values are combined in hyperspectral indices for leaf chlorophyll retrieval and compared against the measured leaf chlorophyll content in the Greater Victoria Watershed District (GVWD), British Columbia (BC). The results demonstrate that the modeled canopy reflectance and AVIRS data are in good agreement for all locations. The regressions of the modified simple ratio $[(\mathbf{R}_{728} - \mathbf{R}_{434})/(\mathbf{R}_{720} - \mathbf{R}_{434})]$ and modified normalized difference index $[(\mathbf{R}_{728} - \mathbf{R}_{720})/(\mathbf{R}_{728} + \mathbf{R}_{720} - 2\mathbf{R}_{434})]$ against chlorophyll content exhibit the best fit using second-order polynomial functions with the root-mean-square errors (RMSE) of 4.434 and 4.247, and coefficients of determination of 0.588 and 0.588, respectively. Larger RMSE are observed when the direct canopy-level retrieval, using canopy-level generated vegetation indices, is considered, suggesting the importance of the proposed canopy-to-level reflectance inversion step in chlorophyll retrieval based on hyperspectral vegetation indices. This approach allows for estimation of leaf level information in the absence of leaf spectra field measurements, and simplifies further applications of hyperspectral imagery at the regional scale.**

***Index Terms*—Chlorophyll, hyperspectral vegetation indices, leaf area index, radiative transfer model.**

Manuscript received September 21, 2012; revised February 10, 2013, May 02, 2013, and May 02, 2013; accepted June 12, 2013. Date of publication July 19, 2013; date of current version December 18, 2013. *(Corresponding author: A. Simic.)*

A. Simic is with G-Eco Research, Toronto, ON M5K 1P2, Canada (e-mail: global@geco-research.com).

J. M. Chen is with the Department of Geography and Program in Planning, University of Toronto, Toronto, ON M5S 3G3, Canada (e-mail: chenj@geog.utoronto.ca).

S. G. Leblanc is with CCRS, Earth Science, Ottawa, ON J1J 2E8, Canada (e-mail: Sylvain.Leblanc@rncan-nrcan.gc.ca).

A. Dyk is with the Pacific Forestry Centre, Natural Resources Canada, Victoria, BC V8T 2C5, Canada (e-mail: Andrew.Dyk@nrcan-rncan.gc.ca).

H. Croft is with the Geography Department, University of Toronto, Toronto, ON M5S 3G4, Canada (e-mail: holly.croft@utoronto.ca).

T. Han is with the BC Geological Survey Branch, Government of BC, Victoria, BC V8T 2C5, Canada (e-mail: Tian.Han@gov.bc.ca).

Color versions of one or more of the figures in this paper are available online at http://ieeexplore.ieee.org.

Digital Object Identifier 10.1109/JSTARS.2013.2271583

I. Introduction

LEAF CHLOROPHYLL content is an important indicator of ecosystem health and sustainability [1], [2] and is the key parameter for quantifying the photosynthetic rate of foliage, and thus plant primary productivity [3], [4]. At fine spectral resolutions, hyperspectral data provide a unique way to retrieve chlorophyll content [4]–[7]. With remote sensing data, two approaches are commonly applied to estimating chlorophyll content: 1) the empirical statistical approach and 2) the inversion of physically based canopy and leaf reflectance models.

1) The empirical approach is based on correlations between hyperspectral indices, derived from reflectance at leaf or canopy level, and chlorophyll content [4]–[10]. Such indices serve as indicators of vegetation stress, senescence, and disease and have been widely used to estimate chlorophyll content. In literature, the focus is on evaluating the reflectance in narrowbands, band reflectance ratios and combinations, and the characteristics of derivative spectra. Different combinations of narrow spectra are analyzed to reduce the effect of some external vegetation parameters and to maximize sensitivity to chlorophyll content. The empirical approach is simple to use and the indices are easy to compute. However, it is a site-, species-, and often, time-specific approach, and it does not account for the complexity of canopy structure. Although biochemical composition controls leaf and canopy reflectance properties, canopy structure [1], in particular, affects canopy reflectance acquired by a sensor [4], [12]–[14]. Leaves in plant canopies, especially in trees and shrubs, are generally highly clumped. Because of canopy features such as phyllotaxy, branch and shoot arrangement and crown structure, forest leaves have more vertical overlap than the case with a random leaf distribution. In literature, statistical estimation of canopy-level chlorophyll content has been done through various methods. Some studies employed the empirical approach, developing a direct statistical relationship between ground-measured chlorophyll content and canopy reflectance measured by a sensor [10]. In other studies, the relationships between reflectance and chlorophyll content were developed at leaf level and scaled up to the canopy level [15],

[16]. Reference [10] evaluated the relationship between hyperspectral indices from imagery and leaf chlorophyll contents obtained from both model-inversion and ground measurement. Reference [10] also compared simulated and measured canopy reflectance to measured chlorophyll content. In any case of chlorophyll retrieval at the canopy level, the canopy structure, soil background, and sun-target-sensor geometry have to be considered. For instance, canopy reflectances can differ among plants that have the same canopy chlorophyll content but different canopy structure [4]. Furthermore, at all sun angles, the leaf clumping decreases the proportion of sunlit leaves and increases the proportion of shaded leaves, affecting the interaction between radiation and vegetation [17]. Many hyperspectral indices are traditional vegetation indices modified for chlorophyll retrieval, which are proposed to minimize the effects of leaf area index (LAI) and soil background and maximize the spectral response to the chlorophyll content [9]. The empirical relationship between leaf reflectance and biochemical contents have been widely used in the studies of [4] and [18]. However, such empirical methods lack temporal and spatial continuity as they have no clear mechanistic basis.

2) The inversion of physically based canopy and leaf reflectance models is another approach to estimate chlorophyll content. In this study, we will focus on inversion of a canopy model. Canopy models use radiative transfer schemes that include a description of canopy architecture. Most sophisticated canopy modeling techniques, used to simulate the radiation transfer regime in a heterogeneous scene such as open forest canopies, are 1) 3-dimensional numerical models such as ray tracing (Flight, Sprint-2, Raytran, and Drat), discrete ordinate (DART), and radiosity models (RGM); and 2) 3-dimensional geometric optical/hybrid models, such as GORT, SGORT, LIM, 5-Scale, and FRT [19], [20]. [20] reported that some 3-dimensional numerical models have matured to the point that they have been successfully validated against field measurements and provide similar results.

Geometric-optical (GO) models are particularly suitable for forest canopies due to their ability to capture structural vegetation parameters. GO models are developed with emphasis on the effects of canopy architecture on radiative transfer [21], where a canopy is represented as a collection of discrete crown entities that cast shadows onto another crown or/and the background [11], [22]. Multiple scattering is a phenomenon that involves reflected radiance after the first collision of light with foliage or background [21], and the simulation of multispectral scattering is an important part of some RT models. This gives rise to hybrid models [21]–[23]. In recent years, a number of GO/hybrid models have been developed to estimate shadow components, canopy reflectance, and bidirectional function (BRDF) (summarized by [24]). Reference [25] combined the G-function and Hot SpoT (GHOST) model to simulate the BRDF of a boreal forest and to describe the canopy geometry based upon the hotspot signature. The Four-Scale Linear Model for Anisotropic Reflectance (FLAIR), a linear kernel-like model based on 4-Scale, has been developed by [26] and used in the studies of [27]. The Forest Reflectance and Transmittance (FRT) model [23], a hybrid directional multispectral model, was combined with the PROSPECT and MCRM models and successfully used in the studies of [28] and [29].

Inversion of the geometric models commonly employs the look-up table (LUT) approach [30]–[32]. The GORT model was successfully inverted to estimate forest cover density [33]. This model was shown to work well for coniferous forests on flat terrain [34]. [35] and [36] successfully inverted 5-Scale in order to calculate leaf reflectance. Reference [25] effectively employed the GOST model in the process of inverting from canopy to leaf.

The main purpose of this study is to test the model inversion approach for the Douglas fir forest in the Greater Victoria Watershed District (GVWD), British Columbia (BC), Canada. This is a top-down approach of estimating leaf reflectance from hyperspectral remote sensing measurements. The simulated leaf reflectances are combined in different hyperspectral indices and correlated with measured chlorophyll content to explore the potential of empirical relationship. This combined *model-based-empirical* approach considers both chlorophyll content and reflectance at leaf level; it reduces possible uncertainties due to 1) LAI variations when chlorophyll content is upscaled to the canopy and/or 2) mixed signals within a pixel when canopy reflectance is often considered as a proxy of leaf reflectance. The leaf reflectance was obtained by the inversion of the 5-Scale model. The top-down approach of estimating leaf reflectance from 5-Scale based on hyperspectral remote sensing data was proposed by [35] and refined by [36]. The intermediate objectives are as follows:

1) to show performance of the geometric-optical 5-Scale model, emphasizing the importance of canopy architecture and multiple-scattering scheme in simulations of canopy reflectance [37]; the performance of the 5-Scale model and the top-down approach of estimating leaf reflectance are tested using the Airborne Visible/Infrared Imaging Spectrometer (AVIRIS) data;
2) to validate the developed concept of inversion of the canopy reflectance model to compute foliage (leaf) reflectance;
3) to examine the relationship between measured leaf chlorophyll content and reflectance indices derived from the simulated leaf reflectance to explore the validity of the concept at leaf level when the impact of canopy structure is removed;
4) to examine the importance and advantage of the canopy-to-leaf reflectance inversion concept over the direct canopy-retrieval approach in the chlorophyll retrieval process based on the empirical approach.

This top-down model inversion approach can be further incorporated into a leaf-model inversion process to estimate chlorophyll content as described by [35] and [36]. For the purpose of better understanding the overall model-based approach, we have included the description of the theoretical approach from [36] as follows.

II. Theoretical Approach

The 5-Scale model is a geometric-optical radiative-transfer model with emphasis on the structural composition of forest canopies at different scales. The model can be used to simulate both closed and open canopy vegetation reflectance, and, thus, it is useful for forests. A general description is as follows (more detailed information about the model can be found in [37]).

1) Tree crowns are simulated as discrete geometrical objects: cone and cylinder for conifers, and spheroid for deciduous species. The nonrandom spatial distribution of trees is simulated using the [38] type A distribution.
2) Inside the crown, a branch architecture defined by a single inclination angle is included [39]. A branch is, in turn, composed of foliage elements (individual leaves in deciduous and shoots in conifer canopies) with a given angle distribution pattern [40].
3) The hotspot is computed both on the ground and on the foliage with gap size distributions between and inside the crowns, respectively.
4) The tree surface created by the crown volume (cone and cylinder, or spheroid) is treated as a complex medium rather than a smooth surface so that shadowed foliage can be observed on the sunlit side and sunlit foliage on the shaded side.
5) A multiple scattering scheme utilizing view factors is used to compute the "shaded reflectivity." This scheme is essential for hyperspectral calculations because it automatically computes a spectrum of the wavelength-dependent multiple scattering factor under given canopy geometry. This makes the 5-Scale truly unique for hyperspectral applications.
6) If canopy and background spectra are available, 5-Scale can output the bidirectional hyperspectral reflectance at any combination of sun and view geometries [40]–[42].

In addition to sunlit foliage and ground components responsible for the reflectance of the canopy under direct solar beam as the sole source of illumination, the model computes shaded foliage and ground components to account for the diffuse radiation from the sky and the multiple scattering. Model parameters are separated into three groups [41] as follows: 1) site parameters-domain-size equivalent to the size of a pixel, LAI, tree density, solar zenith angle (SZA), viewing angle, and relative azimuth angle; 2) tree architecture parameters-crown radius and height, apex angle, needle-to-shoot ratio, foliage clumping index, and typical size of tree foliage; and 3) foliage reflectance and transmittance and background reflectance spectra or band-specific reflectances and transmittance for multispectral simulations. In several studies, the 5-Scale model is presented as an advanced and reliable approach [17].

1) Inversion of 5-Scale Model: The inversion of 5-Scale is based on the multiple scattering scheme incorporated into the model as explained below [35], [36]. As explained by [21], this scheme is based on view factors between sunlit and shaded components of canopy reflectance, including both foliage and background, which allows for the second and higher-order scattering simulations.

The total simulated canopy reflectance (ρ) is a collection of four reflectivity components. They are sunlit foliage and background reflectances $((\rho_{PT}, \rho_{PG})$ and shaded foliage and background reflectances (ρ_{ZG}, ρ_{ZT}). These reflectances are weighted by the fractions/probabilities of viewing the four parts of scenes in the following manner [21]:

$$\rho = \rho_{PT}F_{PT} + \rho_{ZT}F_{ZT} + \rho_{PG}F_{PG} + \rho_{ZG}F_{ZG} \quad (1)$$

where F_{PT}, F_{ZT}, F_{PG}, and F_{ZG} are fractions/probabilities of viewing (from a remote sensor) sunlit tree crown, shaded tree crown, sunlit background, and shaded background, respectively.

The multiple-scattering scheme is the most challenging modeling component. Generally, it causes errors mainly in the NIR regions due to low absorption and high reflectance within vegetation components. The multispectral module within 5-Scale is based on the probability of viewing sunlit and shaded leaves and background using view factors, considering first-, second- and higher order scattering. As described in detail in [21], this scheme is based on various view factors between sunlit and shaded components of both foliage and background which directly depends on the canopy geometry. The multiple scattering scheme incorporates diffuse radiation from the sky. The model includes Rayleigh scattering and default simulations for the atmosphere with no Mie scattering (low aerosol content) allowing for adjustment of the diffuse component (in percent of the direct illumination), which can be estimated with an atmospheric model and added to the default scattering. The 5-Scale model assumes blue sky and minimal atmospheric effects.

Each component (sunlit and shaded reflectance in (1) includes multiple scattering effects. In addition, each component can be treated as a separate entity allowing for the multiple scattering affect to be additive when multiplied with probability factor. This additive nature of the equation allows us to form a factor that incorporates and replaces some or all components, depending on the level of complexity that we choose. As two components are easily measured (sunlit leaf and background), we decided to include shaded components within the M factor. This factor does not represent multiple scattering but rather shaded components of the overall canopy reflectance as shown in (1). In addition to the shaded components (1), the M factor includes the second- and higher orders of reflectivity that affect sunlit foliage (crown).

The sunlit foliage elements can be affected by the second order of scattering from four sources: 1) other sunlit foliage; 2) shaded side of sunlit leaves; 3) sunlit background; and 4) diffused light from the sky. If there is no second-order scattering for the white leaves scenario, the sunlit foliage reflectance would equal measured leaf reflectance, which is then considered in the (2). With this in mind, the M factor is a multiplying factor that contains all these reflectance of second- and higher order of sunlit foliage, in addition to the shaded leaf and background components from (1) [as shown in (2) and (3)].

Thus, the main goal of this approach is to combine, in one factor, all second- and higher order scattering components, which are handled by the model but yet are hard to measure and separate in a given setting. Two sunlit components, sunlit leaf (first-order scattering) and sunlit background, which can be easily measured, are included in the equation to support the concept and to simplify the proposed LUT approach.

In this case, (1) can be expressed as

$$\rho = (\rho_L F_{PT})M + \rho_{PG} F_{PG}. \tag{2}$$

By rearranging (2), the following equation is derived to calculate the M factor [35]:

$$M = \frac{\rho - \rho_{PG} F_{PG}}{\rho_L F_{PT}} \tag{3}$$

where ρ is the canopy-level total reflectance simulated by 5-Scale and ρ_L is measured leaf reflectance, which is an input value.

Other factors in (3) are derived using the 5-Scale model; canopy reflectance (ρ) can be remotely measured, and forest sunlit background reflectivity (ρ_{PG}) is known.

An important change from (1) to (3) is the substitution of ρ_{PT} with ρ_L. ρ_{PT} is the reflectance of sunlit crown, while ρ_L is the sunlit leaf reflectance as measured, for instance, in the integrating sphere in the laboratory. As the sunlit crown surface is complex at different angles to the sun, these two reflectances differ. In the 5-Scale model, the sunlit crown reflectance is calculated based on leaf reflectance, leaf-sun angle, and the probability of viewing the shaded leaves on the sunlit side. To make the inversion simple and feasible, the difference between ρ_{PT} and ρ_L is absorbed into the M factor. This M factor was calculated for each LAI combination, and the LUTs were generated for each land cover type (conifer, deciduous, and regenerating forest). For each LAI combination, the LUTs contained the M factor, total canopy-level reflectance (which was replaced by AVIRIS reflectance in the leaf reflectance estimation; see (4)), sunlit background reflectance, and the viewing fractions for sunlit foliage and background.

Given that the model-driven canopy reflectance (ρ) closely resembles remote sensing data (ρ_{AVIRIS}) and that the M factor for a forest is provided based on (3), then the following equation can be used to estimate leaf reflectance of a pixel representing a forest stand:

$$\rho_L = \frac{\rho_{\mathrm{AVIRIS}} - \rho_{PG} F_{PG}}{M F_{PT}}. \tag{4}$$

The main goal of this study is to show the validity of this approach of using the M factor and the two sunlit fractions in estimating leaf reflectance from stand-level remote sensing.

III. Method and Data

A. Data Description

All data used in this study, except for leaf and background spectra, were provided by the Pacific Forestry Centre (PFC), within the Natural Resources Canada (NRCan). PFC collected both the field and remote sensing measurements over the Greater Victoria Watershed (GVWD) study site. The leaf and background spectra data were collected by the University of Toronto (U of T) within the Campbell River region, located near the study region. Both GVWD and the Campbell River region are situated on Vancouver Island, BC, Canada, within

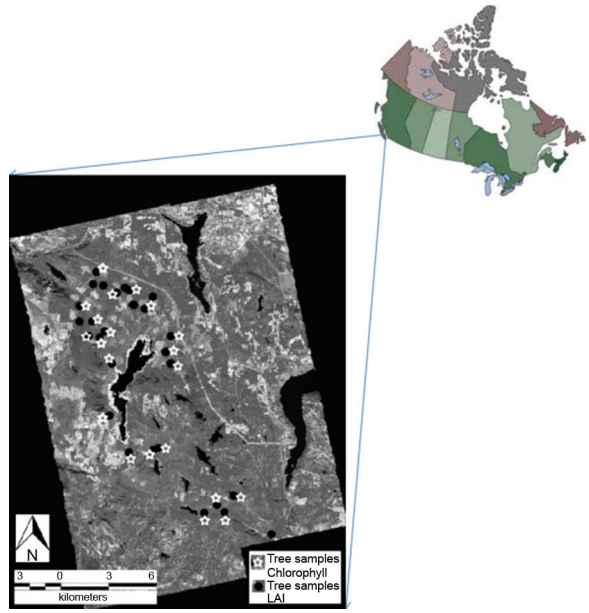

Fig. 1. AVIRIS image for the Greater Victoria Watershed District (GVWD) and given plot locations.

the same eco-region, and it has been assumed that they do not differ significantly in respect to Douglas fir forest and background vegetation species and their structure. The predominant forest species in the study site is Douglas fir (*Pseudostuga menziesii* var. *Menziesii*) [45]. Other species in the area include western hemlock *(Tsuge heterophylla)*, western white pine *(Pinus monticola)*, lodgepole pine *(Pinus Contorta)*, red alder *(Alnus Rubra)*, western redcedar *(Thuja Plicata)*, and arbutus *(Arbutus menziessi)* [45]. The predominant understory species in the study site is salal *(Gaultheria shallon)*.

Remote sensing data included an AVIRIS reflectance image for the GVWD region (Fig. 1). The 20-m airborne hyperspectal AVIRIS data were acquired over the GVWD on September 10, 2001. The data were first atmospherically corrected with the atmospheric correction modeling tool Fast Line-of-sight Atmospheric Analysis of Spectral Hypercubes (FLAASH). The atmospheric corrections were followed by geometric correction and orthorectification with the rational function model. Individual scenes from the flight lines were assembled into a continuous single mosaic image. To eliminate the remaining effects on the spectra, not modeled by the atmospheric correction process, a spectral calibration was performed by forcing the AVIRIS spectra to fit the ground measured spectra at the corresponding locations. Then, the obtained gain and offset were applied to all pixels of the image [45].

The field data provided by PFC were stored in two vector files: a vector point file, containing 54 GVWD plot locations and their extensions (3×3 pixels), and a polygon file, which provided the age and height of trees within each polygon (Fig. 1). The test site boundary was 15 km $\times$ 23 km (Fig. 1). In addition to forest structural parameters, raw LAI measurements, chlorophyll content, and leaf spectra datasets were provided by PFC for 28 plots (Fig. 1). Treetop foliar samples were collected from

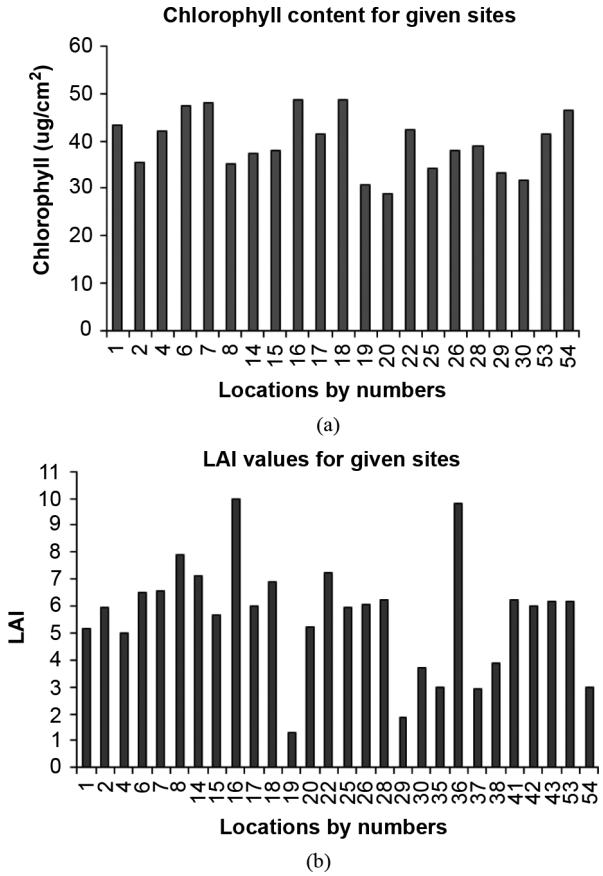

Fig. 2. (a) Chlorophyll content measurements for 21 plot locations. (b) LAI values for 28 plot locations computed by applying the equations of [46] to LAI-2000 raw data.

a helicopter. Ten samples were collected per plot and used for organic analysis, including analysis on chlorophyll a and b, total chlorophyll, moisture percentage of dry weight, and nitrogen percentage for each sample. The organic chemistry analysis was conducted at PFC. Field chlorophyll data [Fig. 2(a)] were used for correlation of reflectance indices and chlorophyll content. LAI-2000 raw data were used to calculate LAI values of plot areas [Fig. 2(b)]. Both chlorophyll and LAI data were collected in summer 2000. More detailed information on the sampling procedure can be found in [45].

The leaf spectra were measured by the Analytical Spectral Devices (ASD) ground spectrometer. The suite of leaf measurements was chosen based on the height and size of trees (dominant, co-dominant, and suppressed), and shoot samples were chosen from three different heights of trees (top, middle, and low) [46]. The analysis included mostly the measurements from the top of a "dominant" tree; it was assumed that they were representative of the forests in the GVWD given that the average height of trees in this area was 33 m, and trees were approximately 55 years old with an average LAI of 6.9 m^2m^{-2}[47]. Following the processing of the ASD measurements, foliage reflectance and transmittance were calculated and used in the analysis. PFC also provided spectra from Douglas fir branch stacks; three sets of data were used for comparison with foliage spectra used in the analysis (both are shown in the results section).

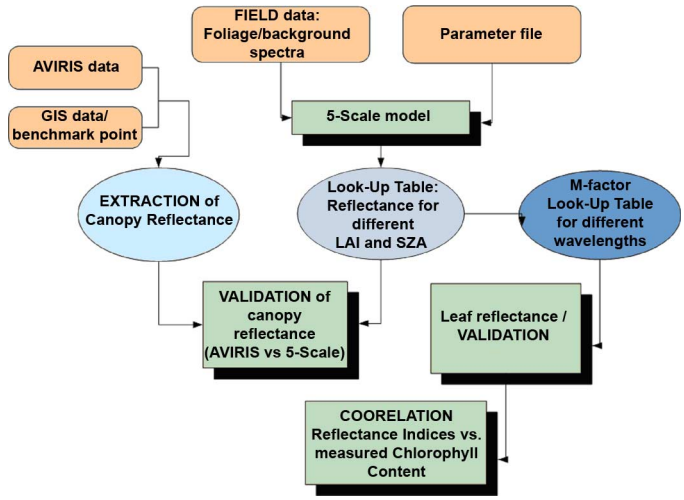

Fig. 3. Major method steps.

B. Description of the Method

Fig. 3 represents the main flow of methods used in this analysis. The two following paragraphs explain the method in more detail.

1) Forward Modeling: The spectral field data from Campbell River were processed using ASD ViewSpecPro version 3.03. Foliage reflectance and transmittance were calculated and then, together with the background reflectance data, used as inputs to the model. Although 5-Scale was modified to calculate foliage reflectance from a leaf model imbedded in the model, availability of the filed measurements allowed us to bypass the leaf model at this stage and, thus, produced more accurate results. The foliage spectra data for Campbell River was compared with the stack spectra of the GVWD region to ensure that the reflectance differences between the two areas were not significant. LAI values of plot areas were calculated using the method of [24] [Fig. 2(a)].

The initial parameterization of the model was based on measurements within the Campbell River site as described by [47]. The parameters were calibrated against a benchmark plot location (Location #14, UTM 10, northing 5381979, easting 449947), which was carefully chosen from the vector data. Both vector data (point and polygon) were overlaid on the AVIRIS data, and the plot location was chosen based on the GIS query to be in accordance with the characteristics of the Campbell River site. The average height of trees was between 30 and 40 m, aged between 40 and 60 years, with an LAI value of 7.0 at the chosen point. These specifications were used in the initial parameterization. In addition, clumping index, needle-to-shoot ratio, and foliage thickness/width ratio, also measured in the Campbell River region, were averaged and used as input parameters for the model. Solar zenith angle for the area was based on the AVIRIS overpass time, and it was calculated to be $\sim 33°$. Validation between canopy reflectance and AVIRIS spectra for the same point was then performed. The model was also run for each reflectance component separately (sunlit and shaded foliage and ground reflectance) to show the contribution of each scene component to the canopy reflectance. The unique fine-tuning of the parameters was then performed over the rest

of the points for which LAI values were provided (28 points). This was done in order to produce the LUTs. Based on this unique parameter file and calculated LAI values, the validation of canopy reflectance for these points was undertaken.

Sensitivity analysis was performed for total canopy reflectance and for sunlit foliage and sunlit ground components and their fractions. The purpose of this analysis was to see how canopy reflectance and its components changed with LAI (1–10) and SZA (10–70).

2) Inverse Model: The M factor, based on the canopy and leaf reflectance as demonstrated in (3), was calculated for the benchmark location first. Estimated leaf reflectance was computed in the next step using AVIRIS data and the M factor in the fashion described in (4). Validation of this process for the benchmark location warranted the inverse canopy model approach. Further validation (for the rest of the points) was performed based on the LUTs, which were produced in the form of text files. The validation was done for all points of interest for given LAI values and SZA of 33°. Some values were interpolated from the LUT.

The first LUT was derived based on sensitivity analysis of the fractions of viewing the four components. It was based on the unique parameter file for LAI ranging from 0.1 to 10 with increments of 0.1 and SZA from 10° to 70° with increments of 10°. Based on this LUT, canopy reflectance modeled for each combination of LAI and SZA, and leaf reflectance measurements, we developed the second LUT, which provides the M factor for given wavelengths for each LAI and SZA combination. The later LUT was created for LAI ranging from 1 to 10 with increments of 1 and SZA from 10° to 70° with increments of 10°. For each combination of LAI and SZA, the wavelength ranges from 400 to 1600 nm with increments of 1 nm. The primary purpose of these LUTs is to invert the hyperspectral remote sensing data in each pixel (treated as a stand) into leaf area reflectance. This approach allows for estimation of leaf level information in the absence of leaf spectra field measurements and simplifies further applications of hyperspectral imagery at a regional scale.

A further step included the computation of leaf reflectance based on AVIRIS data for each point location (3×3 pixels) using the two LUTs. Sunlit background reflectance, in addition, was calculated from the forward mode of the model. Validation of estimated leaf reflectances for all given points was then performed using the given measured leaf reflectance dataset. Table I shows the parameters used for the LUTs. The overall validation of 28 points was shown in the results section. Sensitivity analysis of the M factor was also shown in the results as a function of SZA and LAI.

We explore a number of reflectance indices, including the modified Simple Ratio index (mSR), the modified Normalized Difference index (mND) [48], the Double Difference index (DD), the first derivative-based indices (BmSR and BmND) [9], the Transformed Chlorophyll Absorption in Reflectance Index (TCARI) [49], and the Modified Chlorophyll Absorption in Reflectance Index (MCARI) [50] (see Table II for the reflectance regions included in the equations). Both mSR and mND are modified Simple Ratio ($\mathrm{SR} = \mathrm{R_a}/\mathrm{R_b}$) and Normalized Difference ($\mathrm{ND} = [\mathrm{R_a} - \mathrm{R_b}]/[\mathrm{R_a} + \mathrm{R_b}]$)m

TABLE I
MAJOR PARAMETERS OF A SINGLE PARAMETER FILE USED TO PRODUCE LOOK-UP FOR DOUGLAS FIR STANDS

Stick height (Ha)	18 m
Crown height (Hb)	15 m
Number of trees per ha (D)	500
Radius of crown (R)	2.2 m
LAI	0.1-10
SZA	33.3
Typical foliage element width (Ws)	0.08 m
Element-clumping-index (OMEGA_E)	0.7
Needle-to-shoot-ratio (GAMMA_E)	1.7

TABLE II
RELATIONSHIP BETWEEN SIMULATED LEAF SPECTRAL INDICES (CANOPY SPECTRAL INDICES) AND MEASURED CHLOROPHYLL CONTENT

	Formula	R^2	RMSE
mSR	$(R_{728}-R_{434})/(R_{720}-R_{434})$	0.588 (0.266)	4.434 (5.821)
mND	$(R_{728}-R_{720})/(R_{728}+R_{720}-2R_{434})$	0.588 (0.227)	4.247 (5.822)
BmSR	$(\sigma R_{722}- \sigma R_{502})/(\sigma R_{701}- \sigma R_{502})$	0.349 (0.199)	4.606 (5.834)
BmND	$(\sigma R_{722}- \sigma R_{699})/$ $(\sigma R_{722}+\sigma R_{699}- 2\sigma R_{502})$	0.304 (0.189)	4.673 (6.244)
TCARI*	$3[(R_{700}-R_{670})-0.2$ $(R_{700}-R_{550})*(R_{700}/R_{670})]$	0.391 (0.098)	4.830 (5.964)
MCARI*	$((R_{700}-R_{670})-0.2$ $(R_{700}-R_{550}))*(R_{700}/R_{670})$	0.112	6.160
DD	$(R_{749}-R_{720})/(R_{701}-R_{672})$	0.052	6.130

* We use some indices aimed to be used only at the canopy scale to see whether they performed well at the leaf scale as well.

where an additional spectral range is added in the equation (see Table II) [9]. MCARI was originally designed for canopy cover and generally derived poor results when used at the leaf level; however, we decided to use it in this study [9]. DD index is the difference of the integral of reflectance derivatives. This index is computationally simple and has the advantage to keep the characteristics of hyperspectral indices based on second derivatives [9]. BmSR and BmND are indices based on reflectance derivatives based on mSR and mND [9]. TCARI is a hyperspectral index based on the green spectral region in addition to the red/red edge region [49]. Wavelengths employed in the equations of the indices are commonly the neighboring regions of the chlorophyll absorption maxima (e.g., in the 550 or 700 nm region) as reflectances within these regions are more sensitive to high chlorophyll concentration [9].

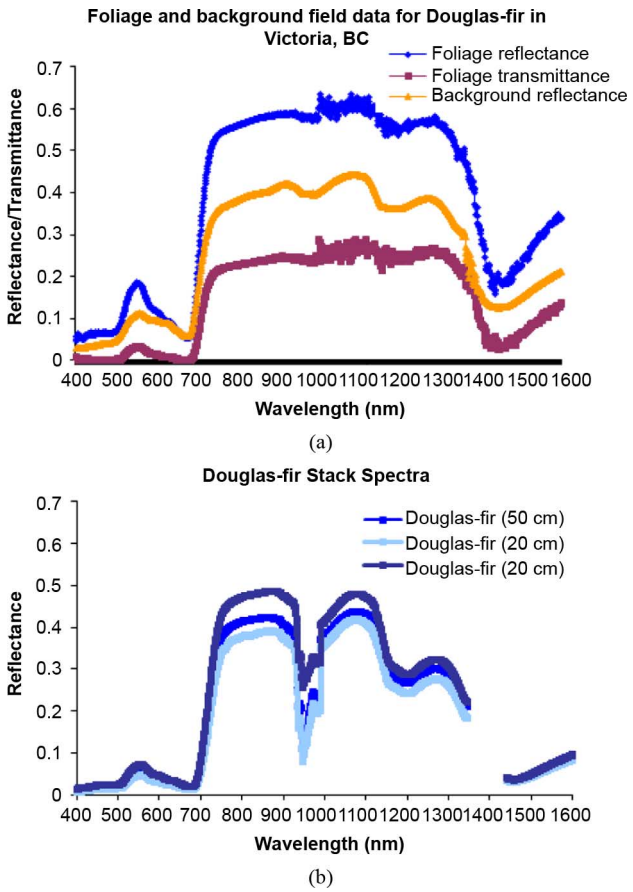

Fig. 4. (a) Input data: Processed leaf spectrum ASD + integrating sphere measurements for the Campbell River region. (b) Douglas fir stack spectra (reflectance) for GVWD.

IV. Results and Discussions

Fig. 4(a) shows the trend of the input data into the model over the wavelength span from 400 to 1600 nm. Although the AVIRIS data provides spectra up to 2400 nm, due to noise and uncertainties during the field measurements, the analysis in this study is limited to 1600 nm. This range satisfies the purpose of this study. Foliage spectra exhibit maximum values of about 0.6 and 0.25 for reflectance and transmittance, respectively. Background spectra exhibit a somewhat higher reflectance value $(\max \sim 0.4)$. However, it was found in this study that the model is more sensitive to variations of foliage reflectance than to variations of foliage transmittance and ground reflectance. For illustration, Fig. 4(b) shows stack spectra for Douglas fir. It exhibits lower values of leaf reflectance for all three measurements (< 0.5) than the foliage spectrum shown in Fig. 4(a). Mutual shadows between stacks of leaves may explain the fact that stack reflectance spectra are lower than the leaf spectra measured inside an integrating sphere. The regions of low reflectance in the stack cases, within the spectral regions 950–990 and 1100–1200 nm, are caused by multiple scattering in the stack, which tends to enhance absorption due to leaf water content. Atmospheric absorption has an additional impact in these spectral regions. These differences suggest that caution should be taken in using stack spectra.

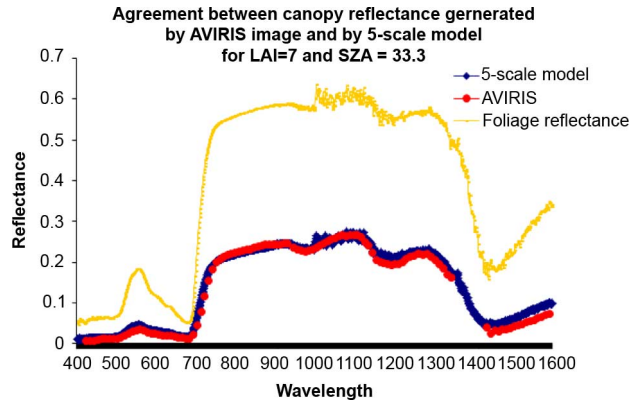

Fig. 5. Agreement between canopy reflectance derived by 5-Scale model and AVIRIS image for the benchmark location (primary location used for the model parameters calibration).

Given that the benchmark location was used as a primary location for the model calibration, Fig. 5 indicates very good agreement of the canopy reflectance derived by the 5-Scale model and extracted from the AVIRIS image for this location. The relationship between the modeled (predictor) and extracted reflectance (response) is defined by the linear regression function $y = 1.024x - 0.01$ and the coefficient of determination $\mathrm{R}^2 = 0.992$, and root-mean-square error (RMSE) is 0.009. The canopy reflectance is considerably lower than the leaf reflectance due to the shadowing effect of the canopy architecture. Thus, the foliage and AVIRIS acquired reflectances, has a strong nonlinear relationship $(\mathrm{R}^2 = 0.990)$ with larger relative differences within the visible range (75% on average) than within the NIR range of the spectrum (60% on average) due to higher multiple scattering in the NIR range.

In addition, it is found that canopy reflectance (not shown) is more sensitive to SZA than to LAI, and it exhibits the highest values for small SZA in both the red and near infrared wavelength ranges.

Good agreement between modeled canopy reflectance and AVIRIS data are observed for other locations of interest as well (R^2 ranges from 0.974 to 0.960; RMSE ranges from 0.011 to 0.022) (Fig. 6). Most discrepancies are due to underestimation of the modeled canopy reflectance, particularly in the near infrared area, between approximately 750 and 950 nm. There is no obvious connection of this trend with LAI values of the locations. The discrepancy can be due to differences in leaf chemistry, and input parameters, tree crown, and height, in particular.

As the main goal of this study was to standardize the LUTs based on one all-location fit parameter file, heterogeneity of the land cover may also cause some discrepancies. Although the region contains $\sim 90\%$ Douglas fir forest, it was observed on the AVIRIS image that the cover types in the windows (3×3 pixels) around some locations of interest were slightly variable. Both average reflectance values of the nine pixels within a window (variability among pixels) and the reflectance of the pixel itself (variability within a pixel) can cause discrepancies at a given spatial resolution.

Fig. 7 shows the reflectance components (sunlit and shaded foliage and background reflectance) for low and high LAI. Due to high open area, high values of sunlit background reflectance

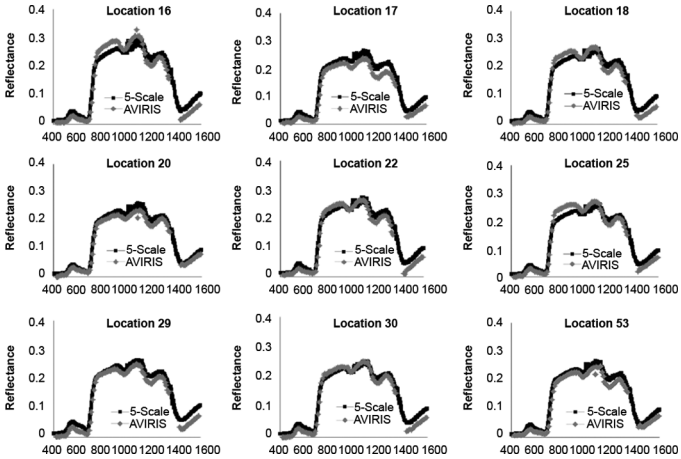

Fig. 6. Agreement between canopy reflectance derived by 5-Scale and AVIRIS data for nine locations. At other locations, the agreements are similar (R^2 ranges from 0.974 to 0.960; RMSE ranges from 0.011 to 0.022).

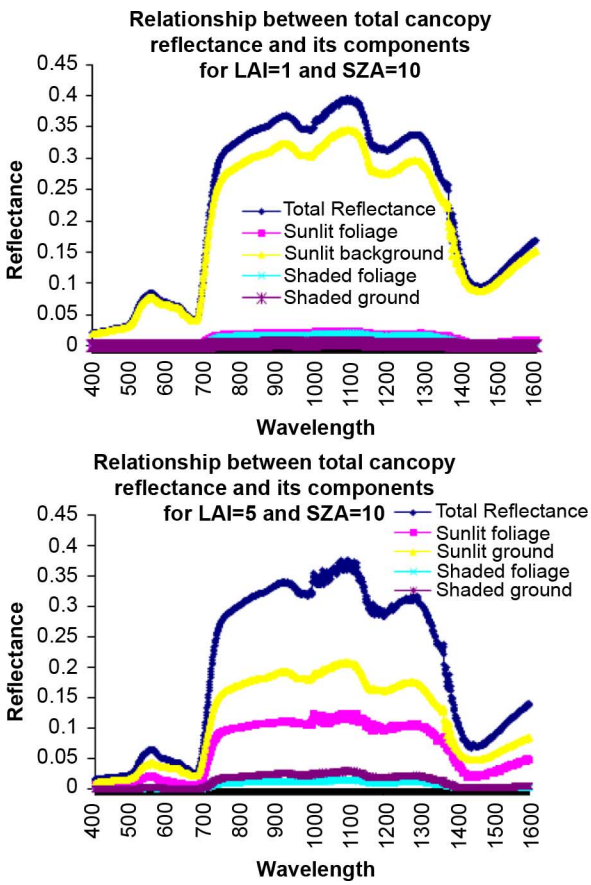

Fig. 7. Variations of the canopy reflectance from various components (sunlit foliage and background and shaded foliage and background) at low and high LAI.

and low values of other reflectance components are seen for low LAI. The sunlit foliage reflectance decreases and sunlit background reflectance increases with increasing LAI.

Fig. 8 indicates that both sunlit foliage and sunlit background reflectance increases with decreasing SZA as the view becomes closer to nadir view. The reciprocal trend of the two components is seen for increasing LAI. As LAI increases, sunlit background reflection decreases.

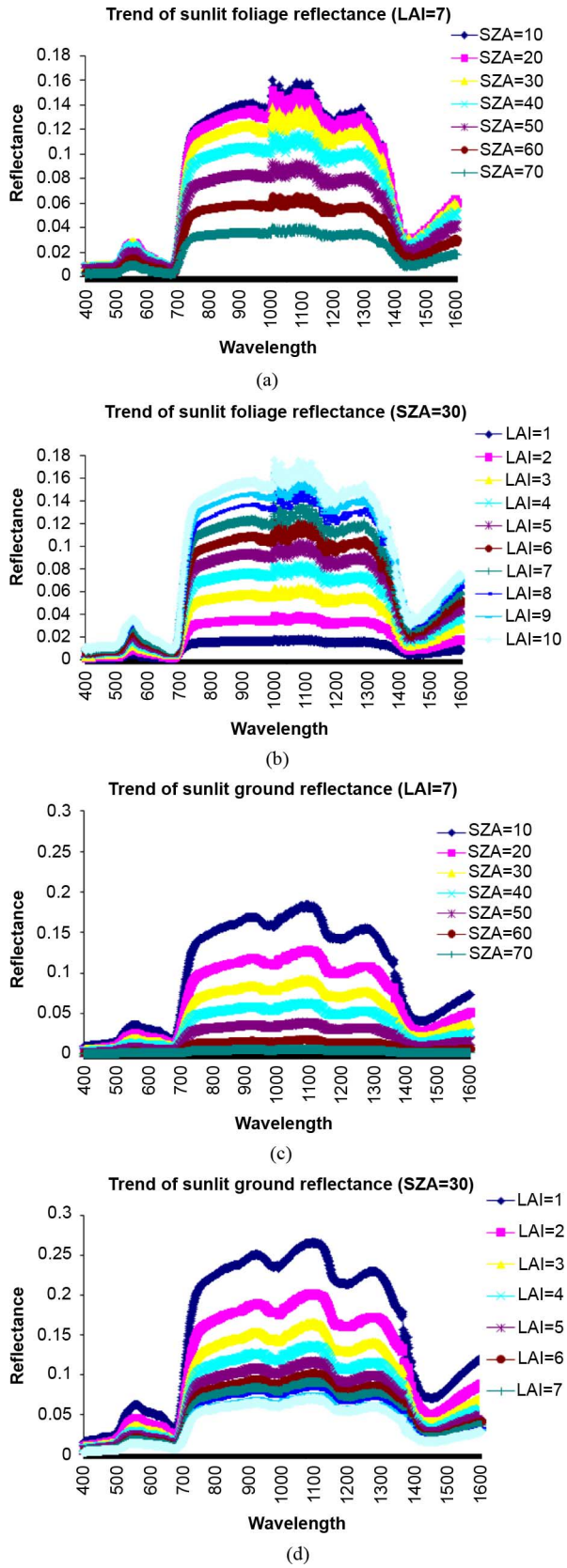

Fig. 8. Sunlit foliage reflectance for (a) different SZAs, for (b) different LAI values. Sunlit background reflectance, for (c) different SZAs, and for (d) different LAI values.

This is directly related to the fractions or probabilities of seeing the scene components (Fig. 9). Probability of seeing

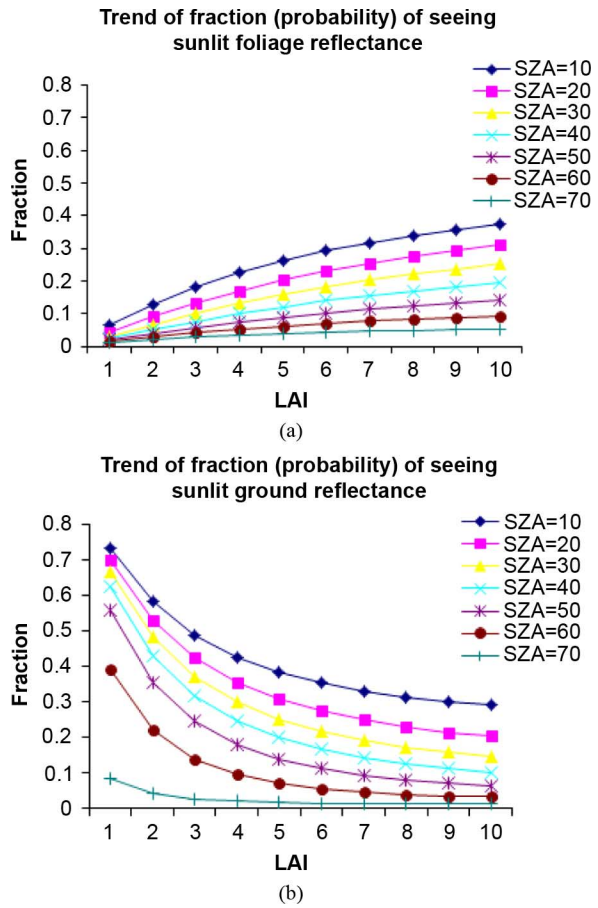

Fig. 9. Trends of the fraction (probability) of seeing (a) sunlit foliage and (b) sunlit background.

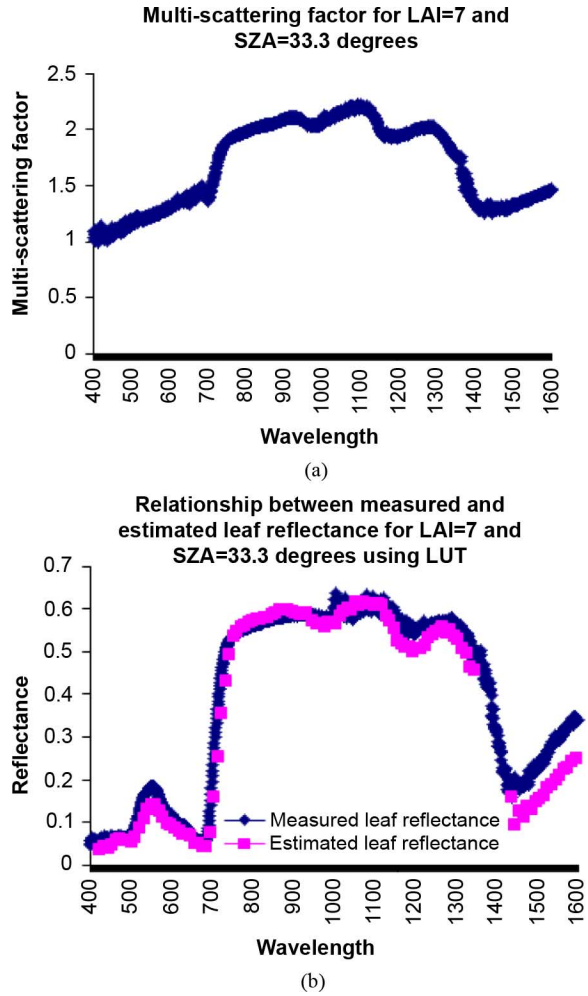

Fig. 10. (a) M factor computed for the benchmark location. (b) Estimated leaf reflectance for the benchmark location and its agreement with the leaf reflectance measurements ($\mathrm{R}^2 = 0.982$; $\mathrm{RMSE} = 0.027$).

sunlit foliage increases while the probability of seeing sunlit background decreases with increasing LAI. Both fractions decrease with increasing SZA.

At this level, the first LUT was produced representing the probabilities of seeing each of the four components as functions of LAI (0.1–10) and SZA (10–70) values.

Fig. 10(a) shows the M factor for the benchmark location based on (3). As M factor incorporates shaded components, its shape follows the general shape of the reflectance over the given wavelength range. Leaf reflectance validation is a very critical portion of this study.

As shown in Fig. 10(b), this approach to the inversion of the canopy model using the M factor is a corroborative approach to calculate leaf reflectance from canopy reflectance. Very strong agreement can be seen between estimated and measured leaf reflectance across both the red and infrared spectral ranges for the benchmark location [Fig. 10(b)]. The coefficient of determination between two reflectances is $\mathrm{R}^2 = 0.982$ and $\mathrm{RMSE} = 0.027$. The modeled leaf reflectance is slightly underestimated within the red edge spectrum.

With multiple scattering the absorption dips should get relatively deeper, or in our M factor, we should see low values where absorption is strong and high values where reflection is strong. In Fig. 10(a), we demonstrate this is the case. The fact that the multiple scattering resembles leaf reflectance spectra in shape demonstrates that we have at least captured the major variance of the multiple scattering effects across the spectrum.

Although no model is perfect, we believe that 5-Scale performed well in this study and that the inversion showed the optimal results. We are very pleased with the results and relatively strong regression as shown by the statistical measures. It is not a surprise that the inversion is less perfect in the NIR region, where models commonly show more uncertainties. Actually, the similar but opposite trend between the errors seen in the validation of the model (at canopy level) and validation of leaf reflectance suggest that the uncertainty are involved more with the 5-Scale than with the inversion process itself.

The second LUT (for M factor) was developed at this stage. The LUT contains the M factor values across the given spectra range for each combination of LAI and SZA. Using both sets of LUTs and AVIRIS data for each given location, leaf reflectance estimation was performed for each site. In addition, the sunlit background data generated by the model was used in the calculations. This component can also be easily measured in the field before being incorporated in the estimation. Fig. 11 shows validation of estimated leaf reflectance for the set of chosen locations. In general, good agreement can be seen for most of the points (R^2 ranges from 0.955 to 0.994; RMSE ranges from 0.036 to 0.085). It is observed that discrepancies within the leaf-reflectance validation (Fig. 11) have similar but opposite

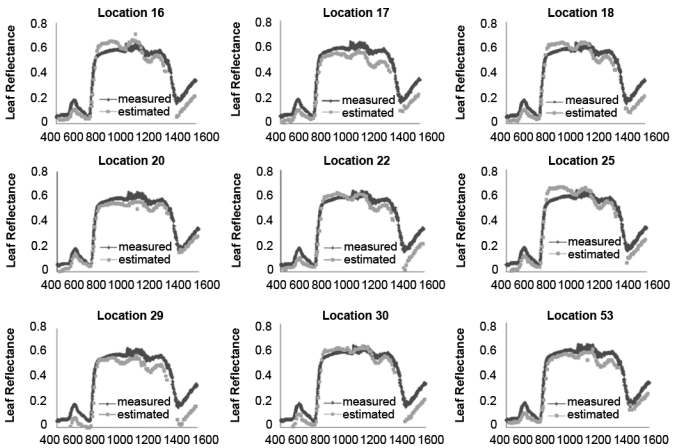

Fig. 11. Agreement between estimated and measured leaf reflectance for nine locations. At other locations, the agreements are similar. (R^2 ranges from 0.955 to 0.994; RMSE ranges from 0.036 to 0.085).

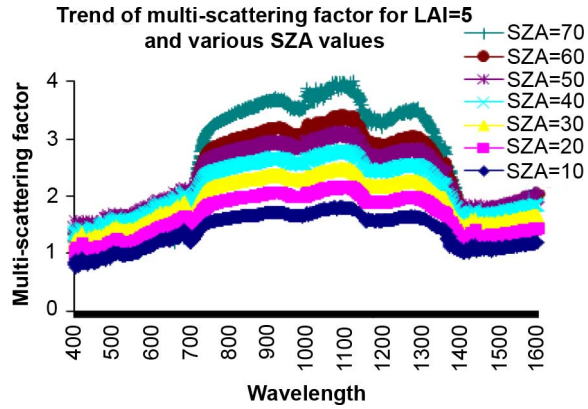

Fig. 12. Variation of the M factor at various SZAs.

trends than discrepancies within the canopy reflectance validation (Fig. 6). This suggests that correct modeling of canopy reflectance is very important in the inversion process. In the visible spectral region, the modeled leaf reflectance is generally underestimated (Fig. 11), while the modeled canopy reflectance is slightly overestimated in most cases (Fig. 6). Variable biochemical contents at canopy and leaf levels may cause these differences. The leaf reflectance is often underestimated within the NIR spectral region, mainly within the water absorption bands. These systematic differences, particularly within the water absorption band at 1450 nm suggest that the inversion approach used in this study has to be improved to account for water content in leaves, and the impact of multiple scattering (within M factor) on leaves with different water content should be explored and corrected.

It should be noted that only one available set of measured leaf reflectance has been used for both calculations of the M factor and validation. However, the errors are not considerable, and we believe that LUTs created in this study provide a reasonable, practical approach to estimating leaf reflectance for Douglas fir forests. The negative leaf reflectances, which sometimes occur at small wavelengths, were observed in cases when AVIRIS reflectance data were higher than sunlit background reflectance. More research should be done to see whether the processing of AVIRIS data has an impact on this error.

Fig. 12 shows a trend of M factor as a function of SZA. It was found that the M factor varies more with LAI (not shown) than SZA values in this study. As has been well described in literature, the various reflectance indices have been correlated with measured chlorophyll content.

Table II shows the result of the regression between different indices used in this study and measured chlorophyll content. The best fits are reached by using mSR and mND [Fig. 13(a) and (b)], for which the root-mean-square errors are 4.434 and 4.247, and coefficients of determination are 0.588 and 0.588 for polynomial models (second order), respectively. Slightly stronger relationships have been observed using power models for the two indices; however, the difference is not significant, and the polynomial models were chosen to keep the consistency with other indices. Reference [51] found a very strong correlation between these indices and chlorophyll content for deciduous forest. The correlations are somewhat better than those in some studies where satellite reflectance is directly used in the empirical approach. Reference [35] reported a stronger correlation with the TCARI/OSAVI index ($R^2 = 0.403$). We did not find significant difference when we incorporated OSAVI within the TCARI/MCARI indices. The reason is that we are dealing with simulated leaf reflectance where structural canopy effects are mostly removed in the top-down approach. The study of [49] and [7] shows a better relationship for the same index for crop canopies and open forest canopies. Somewhat better results are observed between the MTCI index and canopy chlorophyll content as this index better incorporates LAI variations [35]. However, the same relationship is poor when compared with chlorophyll content at leaf level. In cases of open forest, a strong influence of the vegetated understory is the main source of errors [35]. [10] reported better correlation for TCARI and MCARI indices ($R^2 = 0.550$ and 0.470, respectively) than the results shown in this study ($R^2 = 0.391$ and 0.112, respectively). There is no significant difference among RMSE of the "modified" indices (mSR, mND, BmSR, and BmND) in this study (Table II). This is in agreement with [9]; the wavelengths of 434 or 502 nm used in the "modified" indices reduce the effect of differences between specular and internal components of leaf reflectances [9]. However, reflectance derivatives (BmSR and BmND) do not provide better results than their direct reflectance-based counterparts (mSR, mND) as observed in [9] (Table II).

To validate the importance of this step, we compared the results of the canopy-to-leaf inversion with the direct canopy-level retrieval approach, where leaf- and canopy- level Vis are correlated with measured chlorophyll content, respectively.

Larger RMSE are observed when the direct canopy-level retrieval, using canopy-level generated vegetation indices, is considered, suggesting the importance of the proposed canopy-to-level reflectance inversion step in chlorophyll retrieval based on hyperspectral vegetation indices (Table II; the values are placed in the brackets).

The canopy-to-leaf inversion approach has the best regression measurement when leaf-based VIs are compared with the leaf chlorophyll. The findings suggest that the inversion step is

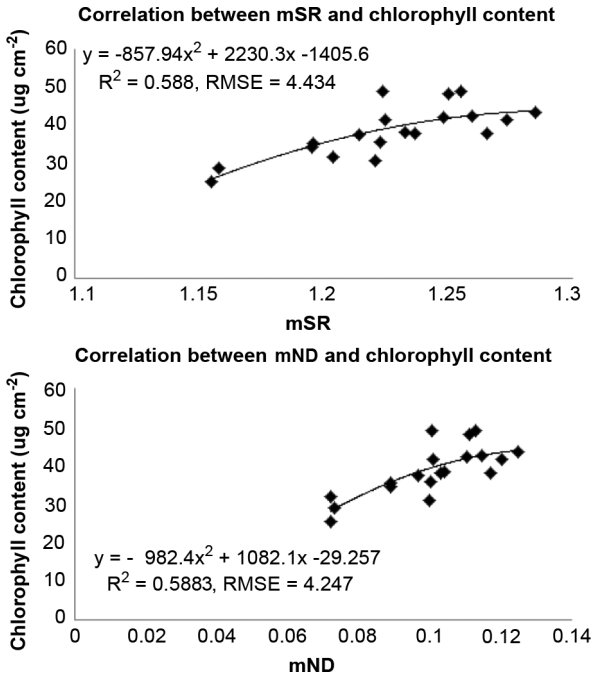

Fig. 13. Regression between two spectral indices and chlorophyll content measurements.

an important in chlorophyll retrieval and that the canopy structure, which we incorporated in the inversion process, is an important step in the empirical approach of retrieving the chlorophyll content at leaf level. Although these preliminary findings deserve additional validation for different study sites, they suggest that the leaf-reflectance based VIs, are more reasonable and more acceptable than the direct canopy-level retrieval using VIs.

The proposed combination of model-based and empirical approaches is an optimal solution to estimating leaf chlorophyll content. Both simulated leaf reflectance and chlorophyll content at leaf level are the best candidates for the empirical relationship as the approach minimizes uncertainties introduced by canopy reflectance that may be caused by LAI variability, background, and observational geometry. The 5-Scale model can provide reasonably good leaf reflectance from satellite imagery by setting proper structural input parameters. The LUT approach considers detailed canopy information and viewing geometry.

Further research should deal with the inversion of the leaf-level model as done by [35] and [36]. Applying this approach, we will be able to incorporate leaf structural components into the estimation of leaf chlorophyll content for each location, and explore whether using the inversion of leaf model for Douglas fir would give a better estimation of chlorophyll content than the results based on the empirical approach in this study. Reference [51] demonstrated that the empirical approach can provide better results than the original (non-modified for leaf thickness) version of PROSPECT leaf model. Reference [35] modified PROSPECT for conifers to reach better results when the inversion of leaf reflectance model PROSPECT was made. The findings in this study show better correlation between the simulated leaf reflectance and chlorophyll content than findings in [36], where the inversion of both canopy and leaf models was performed, and estimated and measured chlorophyll compared.

Although it is hard to pinpoint what may cause this trend in the results, it may be suggested that some additional modifications of the leaf model PROSPECT for conifers are required [35], [36]. Thus, there are several reasons for the proposed combination of model-based and empirical approaches to be considered as optimal in retrieving of chlorophyll content: 1) simulated leaf reflectance minimizes uncertainties introduced by canopy reflectance often used in the empirical relationship with the chlorophyll content at leaf level; 2) the process does not involve the inversion of the leaf radiative transfer model (e.g., PROSPECT), which may introduce additional uncertainties; and 3) the approach allows the leaf level information to be retrieved in the absence of leaf spectra field measurements.

V. Conclusion

The radiative transfer model inversion in this paper is based on the 5-Scale model. We chose this model for several reasons: 1) it is geometric model, and it accounts for the structural components of the canopy in addition to the BRDF effect. In many studies, it is found to be a very reliable model and it provides a unique way for its inversion. We believe that this approach is useful, as differences in the geometric properties of canopies commonly exert more control on the reflection and absorption of radiation than the property of the individual leaves. The top-down inversion of 5-Scale to generate leaf level reflectance from canopy level reflectance performs well when chlorophyll indices at leaf level are compared with leaf chlorophyll content. Leaf reflectance derived from canopy-to-leaf inversion using remote sensing data is a preferable, if not required, approach used in the empirical concept of estimating chlorophyll content at leaf level. In this paper, we demonstrated the importance of the canopy-to-leaf inversion step in chlorophyll content retrieval at leaf level using VIs.

Good agreement between AVIRIS data and modeled reflectance was found for all ground plots. Validation of the measured and estimated leaf reflectance based on the LUTs exhibited good agreement for most of the points. The accuracy of estimated leaf reflectance largely depended on the agreement between remote sensing data and modeled canopy reflectance. Therefore, proper parameterization of the model is crucial for the overall accuracy.

The relatively strong correlation between measured (leaf) chlorophyll content and two spectral indices suggests that the method of calculating leaf reflectance by using the inversion of the canopy level model is a reliable chlorophyll-retrieval method. This approach is advantageous over the direct canopy-retrieval approach, suggesting the importance of the canopy-to-leaf inversion step in chlorophyll retrieval based on VIs. The main advantage of this approach is that it allows for leaf level information retrieval in the absence of leaf spectra field measurements. We expect that the LUTs created in this study could also help remote sensing applications to other conifer species, as the canopy-to-leaf inversions are similar for different conifer species. The ability to estimate leaf level information based on remote sensing data is a large step forward in hyperspectral applications in forestry, including forest health, resources management, and carbon cycle estimation.

ACKNOWLEDGMENT

The authors would like to thank Dr. A. Hollinger of the Canadian Space Agency (CSA) and Dr. D. Goodenough of the University of Victoria for their encouragement of the modeling approach, and for their initial engagement and mutual intention to involve me as a collaborator in their well-planned project. The study was funded through the HUDFEMA project. Further thanks go to Dr. Lisa Zhang and Dr. Oliver Sonnentag, who assisted in collecting the background and foliage spectra data.

REFERENCES

[1] G. A. Carter, "Ratios of leaf reflectances in narrow wavebands as indicators of plant stress," *Int. J. Remote Sens.*, vol. 15, no. 3, pp. 697–703, 1994.

[2] H. K. Lichtenthaler, "The stress concept in plans: As introduction," *Ann. New York Acad. of Sci.*, vol. 851, pp. 187–198, 1998.

[3] F. Ripullone, G. Grassi, M. Lauteri, and M. Borghetti, "Photosynthesis-nitrogen relationships: interpretation of different patterns between pseudotsuga menziesii and populus xeuroamericana in mini-stand experiment," *Three Physiol.*, vol. 23, pp. 137–144, 2003.

[4] A. A. Gitelson, A. Vina, V. Ciganda, D. C. Rundquis, and T. J. Arkebauer, "Remote estimation of canopy chlorophyll in crops," *Geophys. Res. Lett.*, vol. 32, 2005, L08403, doi: 10.1029/2005GL022688.

[5] C. D. Elvidge and Z. Chen, "Comparison of broad-band and narrow-band red and near-infrared vegetation indices," *Remote Sens. Environ.*, vol. 54, pp. 38–48, 1995.

[6] N. M. Broge and E. Leblanc, "Comparing predictive power and stability of broadband and hyperspectral vegetation indices for estimation of green leaf, area index, and canopy chlorophyll density," *Remote Sens. Environ.*, vol. 76, pp. 165–172, 2001.

[7] P. J. Zarco-Tejada, P. J. Miller, G. H. Mohammed, T. L. Noland, and P. H. Sampson, "Scaling-up and model inversion methods with narrow-band optical indices for chlorophyll content estimation in closed forest canopies with hyperspectral data," *IEEE Trans. Geosci. Remote Sens.*, vol. 39, no. 7, pp. 1491–1507, 2001.

[8] P. J Curran, "Remote sensing of foliar chemistry," *Remote Sens. Environ.*, vol. 30, pp. 271–278, 1989.

[9] G. L. Maire, C. Francois, and E. Dufrene, "Towards universal broad leaf chlorophyll indices using prospect simulated database and hyperspectral reflectance measurements," *Remote Sens. Environ.*, vol. 89, pp. 1–28, 2004.

[10] D. Haboudane, N. Tremblay, J. R. Miller, and P. Vigneault, "Remote estimation of crop chlorophyll content using spectral indices derived from hyperspectral data," *IEEE Trans. Geosci. Remote Sens.*, vol. 46, no. 2, pp. 423–437, 2008.

[11] J. M. Chen, G. Pavlic, L. Brown, J. Cihlar, S. G. Leblanc, H. P. White, R. J. Hall, D. R. Peddle, D. J. King, J. A. Trofymow, E. Swift, J. V. der Sanden, and P. K. E. Pellikka, "Derivation and validation of Canada-wide coarse-resolution leaf area index maps using high resolution satellite imagery and ground measurements," *Remote Sens. Environ.*, vol. 80, pp. 165–184, 2002.

[12] P. Lewis, "3D canopy modeling as a tool in remote-sensing research," in *Functional-Structural Plant Modeling in Crop Production*, J. Vos, L. F. M Marcelis, P. H. B de Visser, P. C Struik, and J. B Evers, Eds. Wageningen, The Netherlands: Springer, 2007, pp. 210–229.

[13] Z. Malenovski, E. Martin, L. Homolova, J. P. Gastellu-Etchegorry, R. Zurita-Mila, M. E. Schaepman, R. Pokorny, J. G. P. W. Clevers, and P. Cudlin, "Influence of woody elements of a Norway spruce canopy on nadir reflectance simulated by the DART model at very high spatial resolution," *Remote Sens. Environ.*, vol. 112, no. 1, pp. 1–18, 2008.

[14] J. Verrelst, M. E. Schaepman, and J. G. P. W. Clevers, "A modeling approach for studying forest chlorophyll content in relation to canopy composition," in *ISPRS, XXIst ISPRS Congr., Technical Commission VII, Commission VII, WG VII/1, ISPRS Archives*. Beijing: , Jul. 3–11, 2008, vol. XXXVII. Part B7, pp. 25–30.

[15] D. L. Peterson, J. D. Aber, P. A. Matson, D. H. Card, N. A. Swanberg, and C. A. Wessman, "Remote sensing of forest canopy leaf biochemical contents," *Remote Sens. Environ.*, vol. 24, pp. 85–108, 1988.

[16] F. Zagolski, V. Pinel, J. Romier, D. Alcayde, J. Fotanari, and J. P. Gastellu-Etchegorry, "Forest canopy chemisty with high spectral resolution remote sensing," *Int. J. Remote Sens.*, vol. 17, pp. 1107–1128, 1996.

[17] A. Simic, J. M. Chen, J. Freemantle, J. R. Miller, and J. Pisek, "Improving clumping and LAI algorithms based on multi-angle airborne imagery and ground measurements," *IEEE Trans. Geosci. Remote Sens.*, vol. 48, no. 4, pp. 1742–1759, 2010.

[18] B. Datt, "Visible/near infrared reflectance and chlorophyll content in eucalyptus leaves," *Int. J. Remote Sens.*, vol. 20, pp. 2741–2759, 1999.

[19] B. Pinty, J.-L. Widlowski, M. Taberner, N. Gobron, and M. M. Verstraete, "Radiation transfer model intercomparison (RAMI) exercise: Results from the second phase," *J. Geophys. Res.*, vol. 109, 2004, D06210, 10.1029/2003JD004252.

[20] J.-L. Widlowski, M. Taberner, B. Pinty, V. Bruniquel-Pinel, and M. Disney, "Third radiation transfer model intercomparison (RAMI) exercise: Documenting progress in canopy reflectance models," *J. Geophys. Res.*, vol. 112, 2007, D09111, doi: 10.1029/2006JD007821.

[21] J. M. Chen and S. G. Leblanc, "Multiple-scattering scheme useful for geometric optical modeling," *IEEE Trans. Geosci. Remote Sens.*, vol. 39, no. 5, pp. 1061–1071, 2001.

[22] F. F. Gerard and P. R. J. North, "Analyzing the effect of structural variability and canopy-optical model," *Remote Sens. Environ.*, vol. 62, pp. 46–62, 1997.

[23] A. Kuusk and T. Nilson, "A directional multi-spectral forest reflectance model," *Remote Sens. Environ/.*, vol. 72, pp. 244–252, 2000.

[24] J. M. Chen, "Optically-based methods for measuring seasonal variation of leaf area index in boreal conifer stands," *Agricult. Forest Meteorol.*, vol. 80, pp. 135–163, 1996.

[25] R. Lacaze and J.-L. Roujean, "G-function and hot spot (GHOST) reflectance model application to multi-scale airborne polder measurement," *Remote Sens. Environ.*, vol. 76, pp. 67–80, 2001.

[26] H. P. White, J. R. Miller, and J. M. Chen, "Four-scale linear model for anisotropic reflectance (FLAIR) for plant canopies. Model description and partial validation," *IEEE Trans. Geosci. Remote Sens.*, vol. 39, no. 5, pp. 1072–1083, 2001.

[27] S. G. Leblanc, J. M. Chen, H. P. White, R. Latifovic, R. Lacaze, and J.-L. Roujean, "Canada-wide foliage clumping index mapping from multiangular polder measurements," *Can. J. Remote Sens.*, vol. 31, no. 5, pp. 364–376, 2005.

[28] M. Rautiainen, M. Lang, M. Mottus, A. Kuusk, T. Nilson, Kuusk, and T. Lukk, "Multi-angular reflectance properties of a hemiboreal forest: An analysis using CHRIS PROBA data," *Remote Sens. Environ.*, vol. 112, pp. 2627–2642, 2008.

[29] A. Kuusk and T. Nilson, "Testing directional properties of a forest reflectance model," *J. Geophys. Res.*, vol. 106, no. 12, pp. 011–12, 2001.

[30] B. Combal, F. Baret, M. Weiss, A. Trubuil, D. Mace, and A. Pragnere, "Retrieval of canopy biophysical variables from bidirectional reflectance using prior information to solve the ill-posed inverse problem," *Remote Sens. Environ.*, vol. 84, pp. 1–15, 2002.

[31] Y. Knyazikhin, J. V. Martonchik, D. J. Diner, M. M. Verstraete, B. Pinty, and N. Godron, "Estimation of vegetation canopy leaf area index and fraction of absorbed photosynthetically active radiation from atmosphere-corrected misr data," *J. Geophys. Res.*, vol. 103, pp. 32239–32256, 1998.

[32] M. Weiss, F. Baret, R. B. Myneni, A. Pragnere, and Y. Knyazikhin, "Investigation of a model inversion technique to estimate canopy biophysical variables from spectral and directional reflectance data," *Agronomie*, vol. 20, pp. 3–22, 2000.

[33] W. Ni, X. Li, M. Woodcock, C. E. Caetano, and A. Strahler, "An analytical model of bidirectional reflectance over discontinuous plant canopies," *IEEE Trans. Geosci. Remote Sens.*, vol. 37, no. 2, pp. 1–13, 1999.

[34] C. E. Woodcock, J. B. Collins, V. D. Jakabhazy, X. Li, S. Macomber, and Y. Wu, "Inversion of the li-strahler canopy reflectance model for mapping forest structure," *IEEE Trans. Geosci. Remote Sens.*, vol. 35, pp. 405–414, 1997.

[35] Y. Zhang, J. M. Chen, J. R. Miller, and T. L. Noland, "Retrieving chlorophyll content in conifer needles from hyperspectral measurements," *Can. J. Remote Sens.*, vol. 34, no. 3, pp. 296–310, 2008.

[36] A. Simic, J. M. Chen, and T. Noland, "Retrieval of forest chlorophyll content using canopy structure parameters derived from multi-angle data: the measurement concept of combining Nadir hyperspectral and off-nadir multispectral data," *Int. J. Remote Sens.* , vol. 32, pp. 5621–5644, 2011, doi: 10.1080/01431161.2010.507257.

[37] J. M. Chen and S. G. Leblanc, "A four-scale bidirectional reflectance model based on canopy architecture," *IEEE Trans. Geosci. Remote Sens*, vol. 35, no. 5, pp. 1316–1337, 1997.

[38] J. Neyman, "On a new class of contagious distribution applicable in entomology and bacteriology," *Ann. Math. Stat.*, vol. 10, pp. 35–57, 1939.

[39] J. M. Chen and T. A. Black, "Defining leaf area index for non-flat leaves," *Plant, Cell, Environ.*, vol. 15, pp. 421–429, 1992.

[40] S. G. Leblanc, J. M. Chen, H. P. White, J. Cihlar, R. Lacaze, J.-L. Roujean, and R. Latifovic, "Mapping vegetation clumping index from directional satellite measurements," presented at the 8th Int. Symp. Phys. Meas. Signature Remote Sens., Aussois, France, Jan. 8–12, 2001.

[41] S. G. Leblanc, P. Bicheron, J. M. Chen, M. Leroy, and J. Cihlar, "Investigation of directional reflectance in boreal forests using an improved 4-Scale model and airborne POLDER data," *IEEE Trans. Geosci. Remote Sens.*, vol. 37, no. 3, pp. 1396–1414, 1999.

[42] S. G. Leblanc, J. M. Chen, and J. Cihlar, "Directionality of NDVI in boreal forest: A model simulations of measurements," *Can. J. Remote Sens.*, vol. 23, no. 4, pp. 369–380, 1997.

[43] J. M. Chen, C. H. Menges, and S. G. Leblanc, "Global mapping of foliage clumping index using multi-angular satellite data," *Remote Sens. Environ.*, vol. 97, pp. 447–457, 2005.
[44] F. Canisius and J. Chen, "Retrieving forest background reflectance in a boreal region from multi-angle imaging spectroradiometer (MISR) data," *Remote Sens. Environ.*, vol. 107, pp. 312–321, 2007.
[45] D. G. Goodenough, A. Dyk, O. Niemann, J. S. Pearlman, H. Chen, T. Han, M. Murdock, and C. West, "Processing hyperion and Ali for forest classification," *IEEE Trans. Geosci. Remote Sens.*, vol. 41, no. 6, pp. 1321–1331, 2003.
[46] J. M. Chen, "Optically-based methods for measuring seasonal variation of leaf are indexin boreal conifer stands," *Agricult. Forest Meteorol.*, vol. 80, pp. 135–163, 1996.
[47] G. B. Drewitt, T. A. Black, Z. Nesic, E. R. Humphreys, E. M. Jork, R. Swanson, G. J. Ethier, T. Griffis, and K. Morgenstern, "Measuring forest floor Co_2 fluxes in a Douglas-fir forest," *Agricult. Forest Meteorol.*, vol. 110, pp. 299–317, 2002.
[48] D. A. Sims and J. A. Gamon, "Relationships between leaf pigment content and spectral reflectance across a wide range of species, leaf structures and developmental stages," *Remote Sens. Environ.*, vol. 81, pp. 337–354, 2002.
[49] D. Haboudane, J. R. Miller, N. Tremblay, P. J. Zarco-Tejada, and L. Dextraze, "Integrated narrow-band vegetation indices for prediction of crop chlorophyll content for application to precision agriculture," *Remote Sens. Environ.*, vol. 81, pp. 416–426, 2002.
[50] C. S. T. Daughtry, C. L. Walthall, M. S. Kim, D. C. E. Brown, and J. E. McMurtrey, "Estimating corn leaf chlorophyll concentration from leaf and canopy reflectance," *Remote Sens. Environ.*, vol. 74, pp. 229–239, 2000.
[51] Y. Zhang, J. M. Chen, and S. C. Thomas, "Retrieving seasonal variation in chlorophyll content of overstory and understory sugar maple leaves from leaf-level hyperspectral data," *Can. J. Remote Sens.*, vol. 5, pp. 406–415, 2007.

Anita Simic received the H.B.Sc., M.Sc., and Ph.D. degrees in environmental science and remote sensing from the University of Toronto, ON, Canada, in 1998, 2002, and 2009, respectively.

She is currently working under contract to G-Eco Research, Toronto, ON, Canada. She has been working as a sessional lecturer at the University of Toronto and Ryerson University, Toronto, ON, Canada, since 2005. She was a Sessional Lecturer at Wuhan University in 2009 and a Senior Instructor under contract to the University of Victoria in 2012. Prior to her doctoral degree, she was a professional consultant and project manager in an environmental engineering firm for several years. She also worked at the Canada Centre for Remote Sensing (CCRS). Her research is in the field of remote sensing applications in vegetation science, bioenergy, hydrology, and environment with an expertise in applications of multi-angle hyperspectral imagery.

Dr. Simic has been involved in the IEEE GRS Society since 2002. She was a Guest Editor for the IEEE JOURNAL OF SELECTED TOPICS IN APPLIED EARTH OBSERVATIONS AND REMOTE SENSING and an initiator of the GRSS Chapter in Zagreb, Croatia. She is a Chair of the IEEE GRSS Summer School in Quebec City, Canada (IGARSS'14).

Jing M. Chen received the B.Sc. degree from the Nanjing Institute of Meteorology, China, in 1982 and the Ph.D. degree from Reading University, Reading, U.K., in 1986.

He is Professor in the Department of Geography and Program in Planning at the University of Toronto, ON, Canada. He is Canada Research Chair. His major research interest is in remote sensing of vegetation and quantifying terrestrial carbon and water fluxes. He has published 239 papers in refereed journals, which are cited over 6000 times in the scientific literature.

Dr. Chen serves the International Science Committee of U.S. Fluxnet Research Network, the Science Committee of the Chinese Global Change Program, and the Overseas Expert Panel of the Chinese State Council. He is currently an Associate Editor of the *Journal of Geophysical Research-Biogeosciences*, the *Canadian Journal of Remote Sensing*, and the *Journal of Applied Remote Sensing*. He is a Fellow of the Royal Society of Canada.

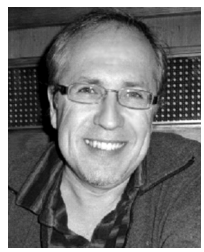

Sylvain G. Leblanc received the B.Sc. degree in physics from the University of Montreal, Montreal, QC, Canada, in 1992 and the M.Sc. degree in atmospheric and oceanic sciences from McGill University, Montreal, QC, Canada, in 1994.

He is currently working towards the Ph.D. degree at the University of Sherbrooke, Sherbrooke, QC, Canada, conducting research on the use of LiDARs to improve forest structure measurements. From 1994 to 1998, he was a Research Associate at the Canada Centre for Remote Sensing (CCRS), Ottawa, ON, Canada, and since 1998, he has been an Environmental Scientist at CCRS, where he co-developed the canopy radiative transfer "5-Scale" and methods and software for *in situ* canopy measurements analysis.

Andrew Dyk received the M.Sc. degree in geography from the University of Victoria, BC, Canada, in 2010 and the Bachelor of Environmental Studies (Hons. Geography) degree from the University of Waterloo, Waterloo, ON, Canada, in 1988.

He is the Deforestation Monitoring Coordinator at the Pacific Forestry Centre, Victoria, BC, Canada, of the Canadian Forest Service, Natural Resources Canada. He continues to be involved in projects to monitor from space all of the forests of Canada, and has been a co-investigator for the experimental satellites EO-1 (NASA), and CHRIS/PROBA (ESA). His remote sensing research was on intelligent hyperspectral data processing, multi-angle image processing, BRDF modeling, automated feature extraction, and data fusion.

Holly Croft received the B.Sc. and M.Sc. degrees in physical geography from the University of Manchester, U.K., and the Ph.D. degree from the University of Exeter, U.K., examining the use of directional reflectance factors and laser techniques for characterising fine-scale soil surface roughness.

She has completed a Postdoctoral Research Fellowship at the University of Basel, Switzerland, focusing on agricultural soil dynamics and remote sensing. She is currently a Postdoctoral Research Fellow at the University of Toronto, ON, Canada. Her main research interests are remote sensing, spatial statistics, leaf biochemistry and canopy biophysical parameters, phenology, and soil science. Her current research projects involve the development and validation of algorithms for modeling leaf chlorophyll content in broadleaf and needle leaf forests and modeling leaf chlorophyll and vegetation productivity in crops.

Tian Han received the Ph.D. degree in computer science from the University of Victoria, BC, Canada.

He is currently a Senior Digital Information Geoscientist with the Geological Survey of British Columbia, Canada. He currently focuses his research on geoscience data management and visualization and remote sensing for geological mapping.